

# ISTITUTO NAZIONALE DI FISICA NUCLEARE

Sezione di Milano

---

INFN/AE-94/14  
11 Maggio 1994

M. Bonesini, S. Gumenyuk, M. Paganoni, A. Pasta, T. Tabarelli, G. Baccaglioni,  
L. Rossi, G. Volpini, M. Pegoraro:

**STUDY IN A HIGH MAGNETIC FIELD OF HAMAMATSU R2149  
TETRODES FOR THE DELPHI STIC CALORIMETER**

**INFN - Istituto Nazionale di Fisica Nucleare**  
Sezione di Milano

**INFN/AE-94/14**  
11 Maggio 1994

**STUDY IN A HIGH MAGNETIC FIELD OF HAMAMATSU R2149 TETRODES  
FOR THE DELPHI STIC CALORIMETER**

**M. Bonesini S. Gumenyuk M. Paganoni A. Pasta T. Tabarelli**

INFN - Sezione di Milano, via Celoria 16, Milano, Italy

**G. Baccaglioni L. Rossi G. Volpini**

LASA (Sezione INFN Milano), via Fratelli Cervi 201, Segrate (MI), Italy

**M. Pegoraro**

INFN - Sezione di Padova, via Marzolo 8, Padova, Italy

**ABSTRACT**

The behaviour of a sample of the magnetic field tolerant phototetrode Hamamatsu R2149-03 has been studied using the high magnetic field provided by the superconducting solenoid SOLEMI-1 at LASA (Sezione INFN Milano). The study has allowed the optimization of their placement inside the new DELPHI luminosity monitor (STIC). Results obtained in magnetic fields up to 4 tesla are also presented.

## 1 INTRODUCTION

The Delphi collaboration has recently proposed a new small angle calorimeter (STIC), see Fig. 1 and <sup>(1)</sup> for more details, to replace the existing luminosity monitor (SAT) <sup>(2)</sup>. It consists of two calorimetric arms located at  $\pm 2.2$  m from the interaction point, divided into two quadrants, 49 sampling layers each, covering the angular region from 29 to 185 mrad in angle, with respect to the beam line. The whole detector will be put inside the magnetic field of DELPHI of 1.2 tesla. Each sampling layer is made of 3.4 mm stainless steel laminated lead as passive material and 3.0 mm polystyrene-based scintillator (1.5% PTP + .05% POPOP) as active media, for a total of 27 radiation lengths. The lead absorber forms a continuous plate, to avoid cracks, while the scintillator plane is formed by tiles optically separated using 120  $\mu m$  thick white TYVEK <sup>1</sup>, which acts as a diffusor. In the two arms the tiles are arranged into half-moons of 8 azimuthal sectors 22.5<sup>o</sup> wide and of 10 radial sectors, for a total of 320 towers. All the mechanics of sampling plates has been carefully surveyed and the measured precision is of about 50  $\mu m$ . For each tower the optical readout is made through WLS fibers (about 1 fiber/cm<sup>2</sup>), orthogonal to the active plates of tiles and grouped together at the back of the calorimeter by a clamp fixed on a supporting plate. The bundles of WLS fibers face in air at 5 mm the 1" tetrodes R2149-03 from Hamamatsu <sup>2</sup>, that will operate inside the solenoidal magnetic field of DELPHI. A charge preamplifier and a high voltage divider are mounted inside the light tight Al support containing each tetrode. The differential output signal is fed via 40 meters long cables to the counting room, where it is processed by the shaper & ADC boards developed for the FEMC, the DELPHI lead glass forward electromagnetic calorimeter.

The construction of STIC is mainly motivated by the goal to have a better measurement of luminosity, both taking advantage of the increase in seen Bhabha cross section due to the smaller beampipe, with respect to what originally foreseen for LEP (reduction of statistical error) and a better control of the geometry and acceptance edges of the used detector (reduction of systematic error).

As testbeam studies of the STIC calorimeter were done with electron beams without a magnetic field, due to available setups, it was found useful to study accurately the behaviour of our photodetector chain (Hamamatsu R2149-03 tetrode + preamplifier) inside a uniform external high magnetic field of 1.2 tesla. This study has helped to define the optimal voltage partition chain (realized afterwards as hybrids), to choose the best orientation of photodetectors with respect to the external magnetic field and optimize the installation of tubes on the four quadrants of the STIC.

We have also studied the behaviour of our HAMAMATSU R2149-03 tetrodes in

<sup>1</sup>registered trademark of DuPont's

<sup>2</sup>for more details see Table 1

very high external magnetic fields up to 4 tesla. These results can be useful for future applications (e.g the “Shashlik calorimeter ” for CMS <sup>(3)</sup> ).

## 2 THE SOLEMI-1 FACILITY

The availability of a large aperture (at least of the order of 15-20 cm) high field magnet was deemed essential for all the tests to be performed. Also a field higher than 1.2 tesla was considered useful for further studies.

After some initial tests with conventional magnets with a much reduced intercoil gap, we exploited the SOLEMI-1 <sup>(4)</sup> facility at LASA laboratory (INFN Milan) that satisfies all the above requirements, having a 535 mm wide useful aperture at *room temperature*, and an operating field up to 8 teslas. The field homogeneity in a volume  $20 \times 20 \times 10$  cm<sup>3</sup> around the center is sufficient for our purposes, being better than 1%, as can be seen from Fig. 3.

The superconducting magnet, whose section is shown along with the experimental apparatus in Fig. 2, is composed of two NbTi solenoidal coils operated in a liquid Helium bath at about 4.2 K. An intermediate thermal shield set between the liquid Helium vessel and the vacuum chamber and cooled by liquid nitrogen adsorbs most of the thermal radiation coming from the room temperature surroundings. The vacuum inside the cryostat is kept below  $10^{-6}$  torr by means of a continuously acting diffusion pump (not shown in the drawing). The main characteristics of the magnet are summarized in table 2.

The operating cycle of the magnet requires about ten days for cooling down from 300 K to 4.2 K and, when operated, it consumes about  $17$  l·hour<sup>-1</sup> of liquid helium. For these measurements the field was kept on for 164 hours, during a period of 21 days.

## 3 EXPERIMENTAL SETUP

About 340 Hamamatsu tetrodes R2149-03 have been delivered in batches, during the first half of 1993, to equip the electronic readout chain of the DELPHI STIC luminosity monitor.

For the tests inside the SOLEMI-1 magnetic field at LASA, they have been mounted inside an aluminium or brass optically tight support, containing a JFET preamplifier in charge sensitive configuration.

Performances have been optimized for the tetrode capacitance giving an ENC of 250 electrons when filtered with gaussian shaping time of 500 ns. The sensitivity is  $.23$   $\mu V$ /electron with a rise time of 20 ns followed by an exponential ( $\tau \sim 10$   $\mu s$ ) fall. The differential output can drive twisted pair cables (or two 50 ohm coaxial cables) with a dynamic range of 15 bits, while consuming 200 mW from  $\pm 6V$  supplies (for more details see <sup>(5)</sup> ).

In part of our tests (optimization of the voltage divider chain) we have used separate HV inputs for the two gain stages of tetrodes, in order to vary at will the partition ratio. The output from the preamplifier was fed into a NIM shaping amplifier <sup>3</sup> and then into a NIM Charge-amplitude-time converter <sup>4</sup> connected to a multichannel analyzer <sup>5</sup>, where a dedicated microprocessor did the peak search analysis needed. Green LED's <sup>6</sup>, driven by a light diode driver <sup>7</sup>, were used as light sources. The LED driving pulse was set to about 50 ns width, with a repetition rate of 1 KHz.

As only relative measurements on a short timescale (gain ratios inside/outside magnetic field) were done, we were not compelled to set up a complicate monitoring system for the stability on a long time scale of our system. We have checked that our system had a maximum drift in time of less than 1% on the measurement timescale.

In the first part of our tests (optimization of the voltage divider chain, angular dependence of gains) single photodetectors were precisely positioned inside the SOLEMI-1 magnetic field with an anticorodal mechanical support, that allowed to test different  $\theta$  angles between the magnetic field direction and the tetrode longitudinal axis. Moreover the tetrodes could be rotated around their longitudinal axis in the range  $0^0 \leq \phi \leq 360^0$ , in such a way that  $\phi = 0^0$  corresponded to the same position of the first dynode pin for all tubes. Both  $\theta$  and  $\phi$  could be defined at better than  $\pm 1^0$ . In the second part of our tests groups of photodetectors (up to 19/group) were mounted on a platform that could be placed precisely at a fixed  $\theta$  angle inside the magnet, to use as much as possible of the available magnet volume.

## 4 RESULTS

### 4.1 Optimization of the voltage divider chain

As a first step, the voltage divider chain, to be realized with hybrids, was optimized assuming a fixed voltage input of - 1000 V for the cathode (K) and tuning the voltage inputs for the two dynodes (DY1,DY2). The optimization was done inside a 1.2 tesla magnetic field from SOLEMI-1 and results are shown in fig. 4 for a typical tetrode. Best results were obtained at:

$$V_K = -1000 \text{ V}$$

$$V_{DY1} = -550 \text{ V}$$

$$V_{DY2} = -200 \text{ V}$$

<sup>3</sup>module N470 from Ortec

<sup>4</sup>module 7422 from Silena,Milano.

<sup>5</sup>MCA Silena 8938

<sup>6</sup>type HLMP-3502 from Hewlett-Packard

<sup>7</sup>CERN type N4168

in agreement with results found also without magnetic field. Fig. 5 shows the mounting of the voltage divider chain and preamplifier electronics inside the optical tight support used for the STIC tetrodes. In all the following, results were obtained using the final high voltage hybrids.

## 4.2 $\theta$ - dependence of tetrode gains

It is a well known fact that, inside a high magnetic field, the gain of triodes and tetrodes, even if field tolerant, is greatly reduced. For a sample of about 280 R2149-03 Hamamatsu tetrodes Fig. 6 shows the gain distribution at zero field (as from Hamamatsu datasheets) and at 1.2 tesla, after measuring the ratio of gain inside and outside magnetic field for the same tubes. We see a strong reduction in absolute gain (from  $\sim 30$  to  $\sim 19$ ). The absolute value of this reduction is also a function of the way the photocatode of tetrodes are illuminated (collimated spot or diffused green light ): in our tests we have tried to simulate at our best the situation to be found in the real experimental setup, where a bundle of 1 mm WLS fibers (SCSF Kuraray Y7, emission peak at  $\sim 500$  nm, aluminized at one end) is positioned at about 5 mm from the photocatode edge.

Due to the effect of the magnetic field on the accelerated electrons inside the tetrodes we can expect a marked dependence of the relative gain as a function of the  $\theta$  angle, as well as also a less marked dependence on the azimuthal orientation  $\phi$  (mainly connected to the fine mesh structure of the anode and the first dynode).

Fig. 7 (a), at a field of 1.2 tesla, shows the dependence from the  $\theta$  angle for some individual tubes. The average profile histogram, for a test sample of 29 tubes, is shown in Fig. 7 (b). An increase of gain (about 20%) is evident at an angle  $\theta \simeq 15^\circ$ . At the expense of a more complicated mechanical support for the tetrodes, we decided to mount them at this angle with respect to the DELPHI magnetic field (parallel to the beam axis) to maximize gains and be in a stable region.

The decrease of the relative gain  $G(\theta)/G(\theta = 0)$  at large values of  $\theta$  is connected to electron losses: large angle electrons fall out the grid surfaces and are lost. This deflection of particle trajectories is also responsible of the enhancement of the relative gain up to a certain value of  $\theta$ . Extensive Monte Carlo studies for fine mesh photo-multipliers in magnetic field, from which we can derive useful informations for our case (tetrodes) were done in reference <sup>(6)</sup>.

## 4.3 $\phi$ -dependence of tetrode gains

For a magnetic field  $B=1.2$  tesla and a fixed value of the  $\theta$  angle between the tetrode axis and the magnetic field direction, a  $\phi$  scan of  $180^\circ$  around the tetrode longitudinal axis was performed in steps of  $\sim 26^\circ$ . The relative variation of the gain  $G$  with respect

to the value at  $\phi = 0^0$  is shown in Fig. 8 (a) for a typical tetrode and in Fig. 8 (b) as an average profile plot. For individual tubes variation up to  $\pm 5\%$  were observed. We were thus compelled to keep track also of the  $\phi$  orientation of individual tubes in the mounting on the STIC detector.

#### 4.4 Dependence of tetrode gain from the magnetic field $B$

Magnetic fields may deflect primary and secondary electrons from their normal trajectories and cause losses in gain. These effects are greatly reduced in fine mesh tubes with a reduced number of multiplication stages, such as the R2149-03 Hamamatsu tetrodes.

Fig. 10 shows, as a function of the magnetic field  $B$ , the relative gain for two typical tubes. Going to about 4 tesla we have a reduction of about a factor 3 in gain, with marked differences from tube to tube. The behaviour, as a function of the  $\theta$  angle is shown, for different magnetic fields, in Fig. 10 too. Normalizing the relative gain at  $\theta = 0^0$  at 1, we see that the shape of the  $\theta$  behaviour of each tube seems to be independent of the magnetic field value and shows qualitatively a kind of "universal behaviour". For a sample of 18 tubes Fig. 9 shows the profile histogram (up to 4 tesla) of the relative gain as a function of magnetic field at  $\theta = 15^0$ .

## 5 CONCLUSIONS

The behaviour of a sample of magnetic field tolerant Hamamatsu R2149-03 tubes has been studied and the results were used to optimize their mechanical mounting inside the DELPHI STIC detector. The results obtained at high magnetic field, around 4 tesla, show that their use may be feasible inside very high magnetic fields.

### Acknowledgements

We are greatly indebted to T. Camporesi, CERN and A. Pullia and P. Negri, University of Milano, for the great help and many discussions on the argument and to W. Bonivento and P. Ferrari for having taken part in some of the measurements. We acknowledge the excellent work of the technicians of INFN Milano F. Chignoli, L. Leoni, R. Mazza, G. Cartegni, L. Gini, A. Leone and D. Pedrini in the preparation of the test setup, the running of the SOLEMI-1 test facility and the great help in the execution of these measurements and of the technician of INFN Padova L. Castellani in the realization of the electronic setup and mounting of all tetrodes.

photocathode type	bialkali
useful photocathode diameter	22 mm
no. of dynodes	2
anode dark current	~ .1 nA
Q.E. at 390 nm	~ 20%
typical gain (B=0 tesla)	~ 30

**TABLE 1:** Characteristics of the tetrode Hamamatsu 2149-03

		<i>inner section</i>	<i>outer section</i>
inner radius	(mm)	317	377.4
outer radius	(mm)	355.4	455.8
length	(mm)	907.2	910.2
insulation thickness	(mm)	0.2	0.2
winding unit cell	(mm)	3.2 × 4.8	2.8 × 4.1
cross section	(mm <sup>2</sup> )	15.36	11.48
number of layers		12	28
number of turns		2268	6216
section inductance	(H)	1.82	19.2
total inductance	(H)	30.44	
magnet current at 8 T	(A)	905	
non copper $J_c$	(A/mm <sup>2</sup> )	715	1550
overall $J_c$	(A/mm <sup>2</sup> )	58.9	78.8
max. voltage to ground	(kV)	2	

**TABLE 2:** SOLEMI-1 main parameters



## REFERENCES

- (1) The DELPHI Collaboration, "Proposal for the replacement of the Small Angle calorimeter of DELPHI", CERN/LEPC/92-Add 1, May 1992  
A. Benvenuti et al., "Prototype design, construction and test of a Pb/scintillator sampling calorimeter with wavelength shifter optic readout", CERN-PPE/92-212, December 1992  
A. Benvenuti et al., "Status of the DELPHI Small angle Tile Calorimeter project", to be published in the HEP EPS 93 Conference proceedings, Marseille, July 1993  
A. Benvenuti et al., "STIC the New DELPHI Luminosity Monitor", to be published in the IV International Conference on Calorimetry in HEP proceedings, Elba, September 1993.
- (2) The DELPHI Collaboration, "The DELPHI detector at LEP", Nucl. Instr. and Meth. **A303** (1991) 233-276  
A. Klovning, "Small angle tagger (SAT) for DELPHI/LEP", 1990, Proceedings Fermilab, Batavia 1990,415-428.
- (3) CMS Collaboration, CMS Letter of Intent, CERN/LHCC 92-3, October 1992  
J. Badier et al., preprint X-LPNHE/93-2  
J. Badier et al., preprint X-LPNHE/93-4
- (4) E. Acerbi et al., "SOLEMI-1, a 8 tesla, 535 mm Room Temperature Bore, Superconducting Solenoid", INFN/TC-92/23, October 1992.
- (5) M. Pegoraro et al., DELPHI note in preparation, 1994.
- (6) G. Barbiellini et al., "A Simulation Study of the Behaviour of Fine Mesh Photomultipliers in Magnetic Field", INFN/AE-93/27, December 1993.

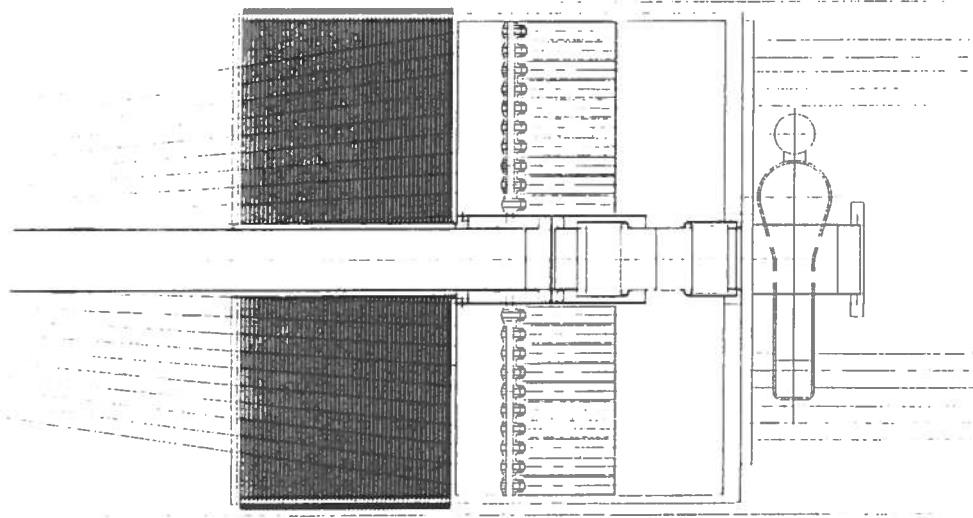


FIG. 1: Layout of one arm of the DELPHI STIC luminosity monitor: vertical section, showing the beampipe, the calorimeter sampling planes and the tetrode boxes

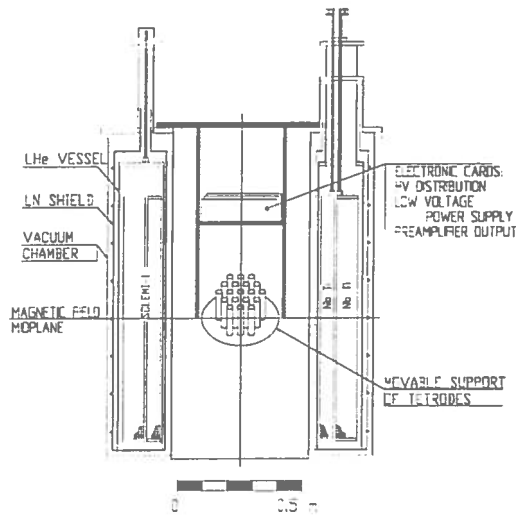
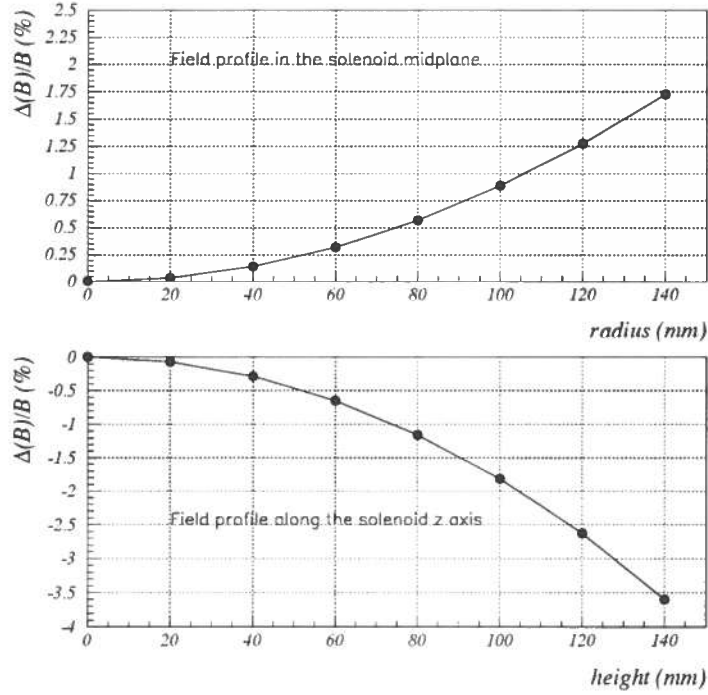
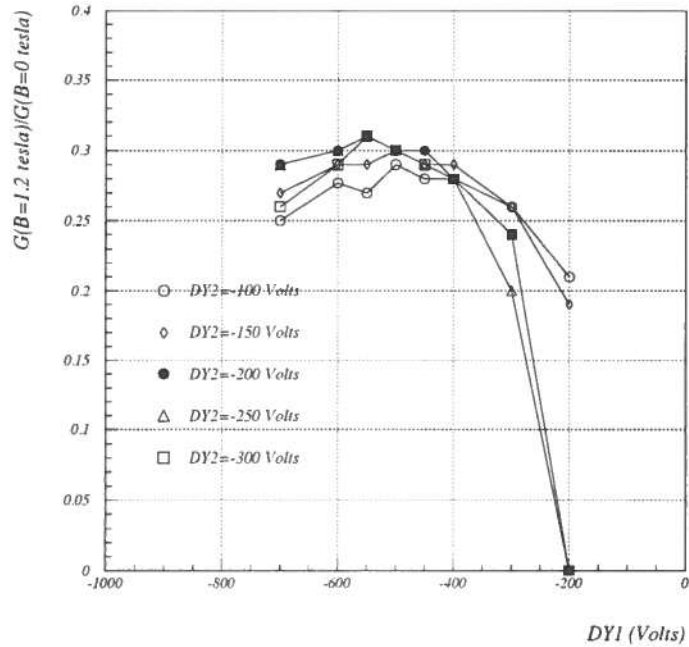


FIG. 2: Cross section of the superconducting solenoid SOLEMI-1 at LASA, with inserted the platform for holding the group of tetrodes



**FIG. 3:** Field profiles inside the bore of SOLEMI-1: (a) radial profile in the midplane; (b) profile along the solenoid z-axis.



**FIG. 4:** Dependence of the gain  $G$  from the chosen partition chain at 1.2 tesla (the normalization at  $B=0$  tesla was done setting the partition chain at  $K=-1000$  V,  $DY1=-550$  V and  $DY2=-150$  V).

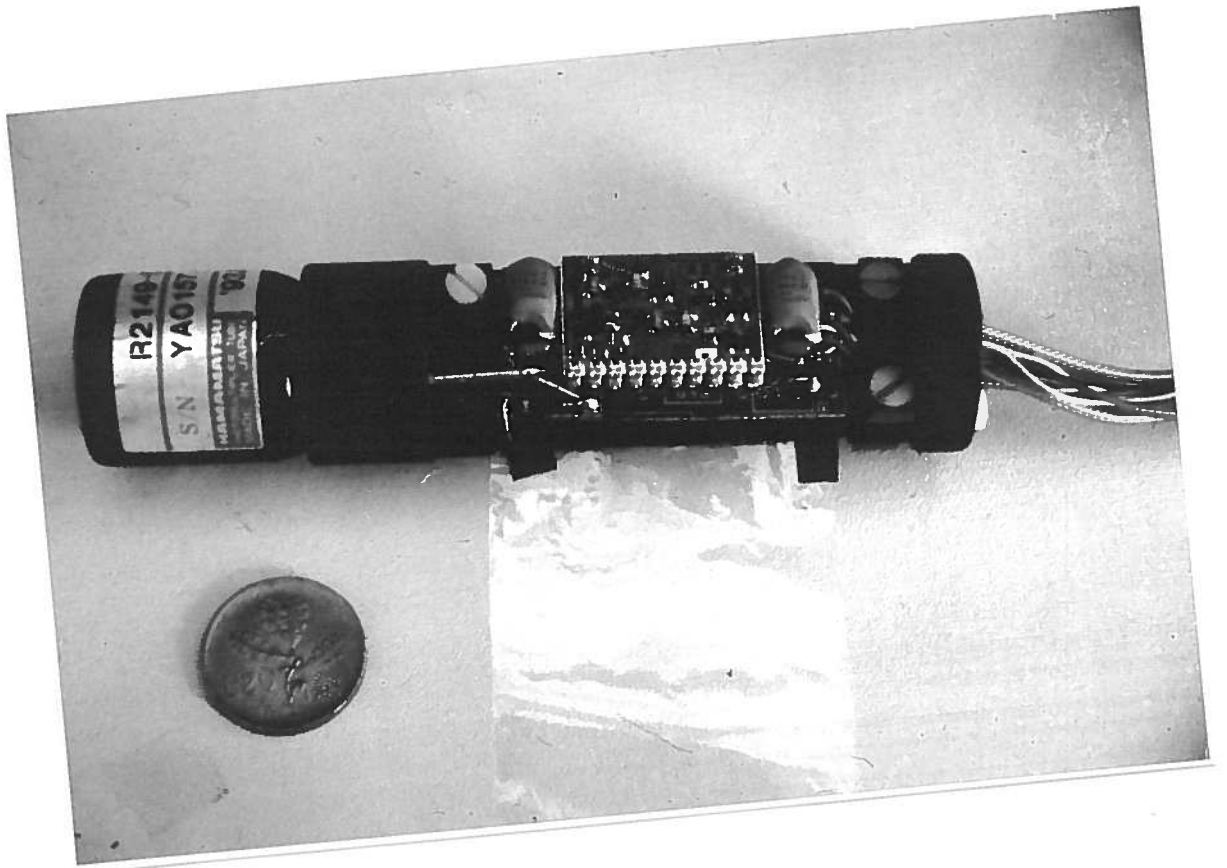
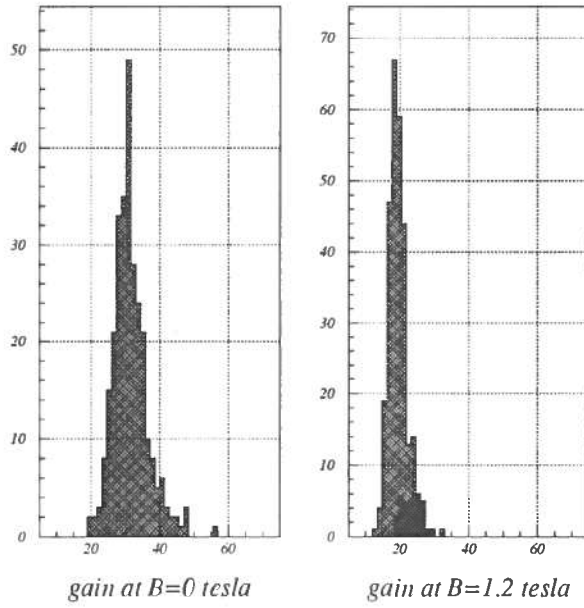
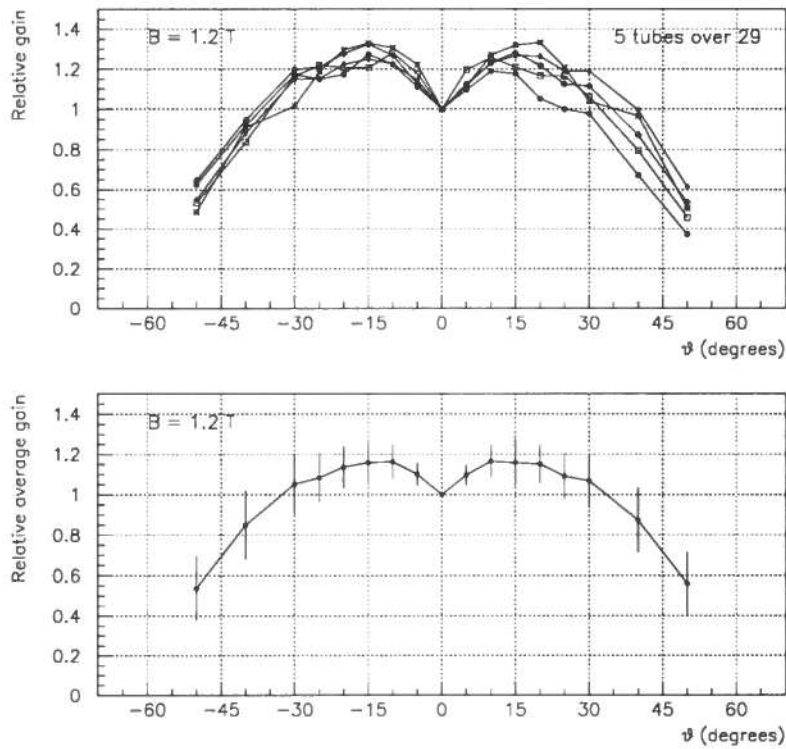


FIG. 5: Voltage divider chain and preamplifier electronic mounted on a STIC tetrode base



**FIG. 6:** Distribution of gains for a sample of about 280 R2149-03 Hamamatsu tetrodes at 0 tesla (a) and 1.2 tesla ( $\theta = 15^\circ$ ) (b)



**FIG. 7:** Distribution of gains as a function of  $\theta$  for a sample of 29 R2149-03 Hamamatsu tetrodes at 1.2 tesla: individual tubes (a), average profile (b) (error bars show rms spreads)

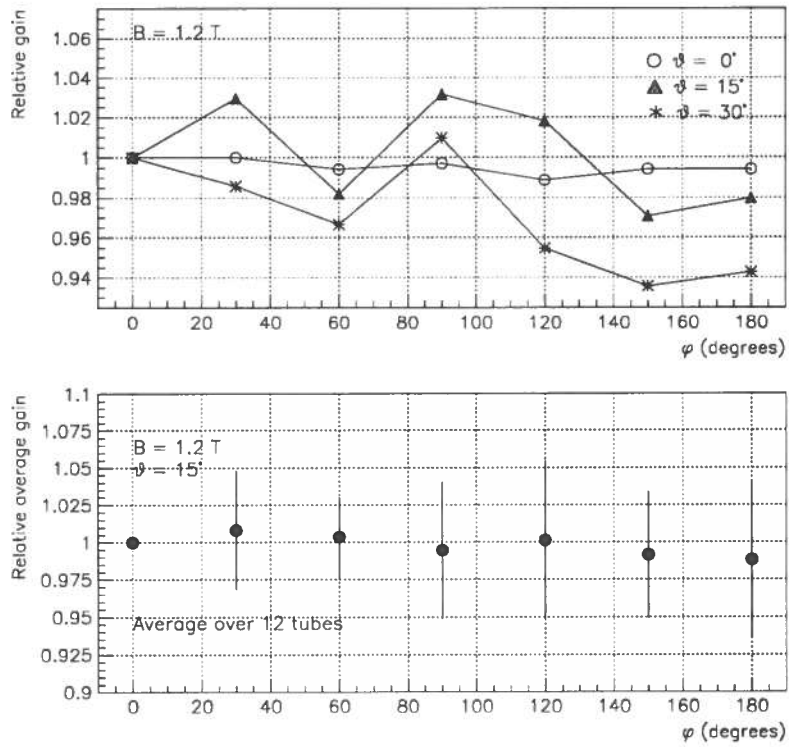


FIG. 8: Distribution of gains as a function of  $\phi$  for a sample of R2149-03 Hamamatsu tetrodes at 1.2 tesla: typical tube at various  $\theta$  angles (a), average profile at  $\theta = 15^\circ$  (b) (error bars show rms spreads)

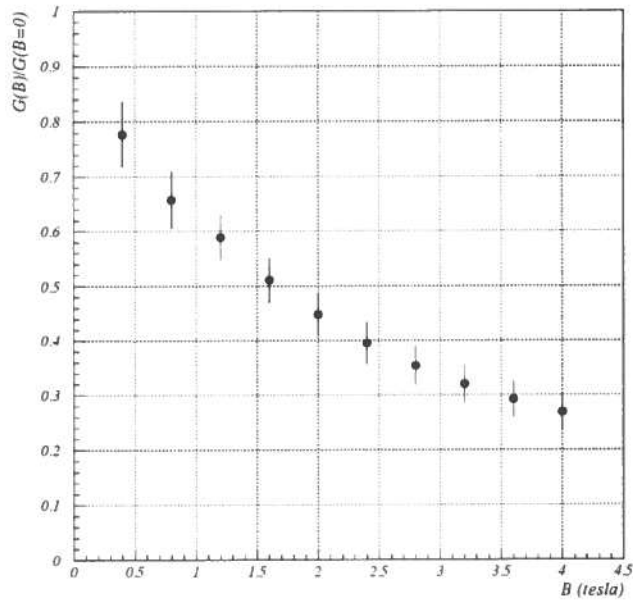


FIG. 9: Profile histogram of the relative gain  $G(B)/G(0)$  as a function of the magnetic field  $B$  (at  $\theta = 15^\circ$ ) for a sample of 18 tetrodes (error bars show rms spreads)

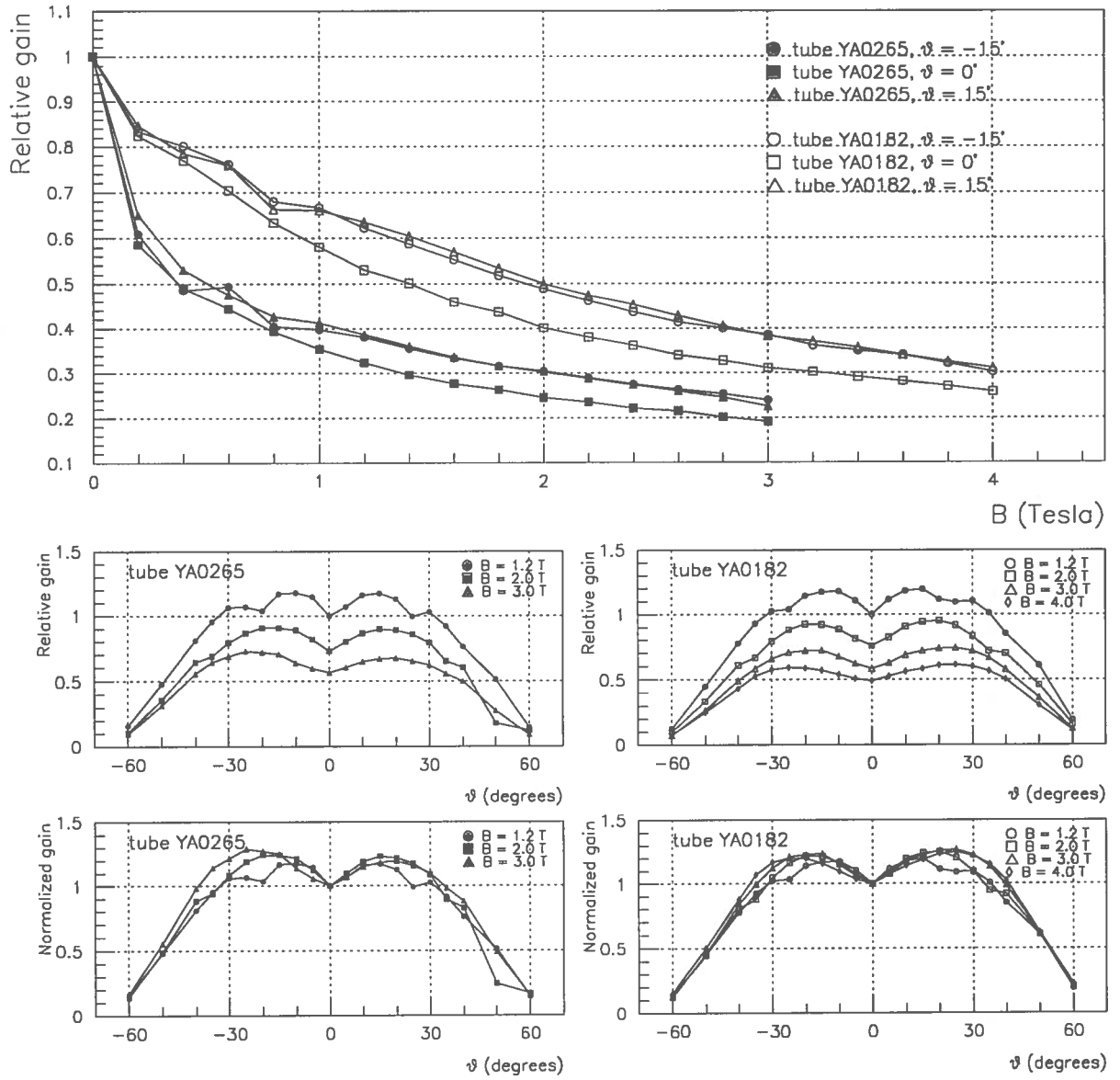


FIG. 10: Relative gain  $G(B)/G(0)$  as a function of the magnetic field  $B$  (a) and as a function of  $\theta$  (b) for different values of  $B$